DØ Note 5176-CONF

Search for Third Generation Leptoquarks in $p\bar{p}$ collisions at $\sqrt{s} = 1.96$ TeV

The DØ Collaboration
URL http://www-d0.fnal.gov

(Dated: July 12, 2006)

We report on a search for charge 1/3 third generation leptoquarks (LQ) produced in $p\bar{p}$ collisions at $\sqrt{s} = 1.96$ TeV using the D0 detector at Fermilab. Third generation leptoquarks are assumed to be produced in pairs and to decay to a tau neutrino and a b quark with branching fraction B. We present preliminary results using an integrated luminosity of 310 pb^{-1}. We place upper limits on $\sigma(p\bar{p} \to LQ\overline{LQ})B^2$ as a function of the leptoquark mass M_{LQ}. Assuming $B = 1$, we exclude at the 95% confidence level third generation leptoquarks with $M_{LQ} < 219$ GeV/c^2.

Preliminary Results for Summer 2006 Conferences

I. INTRODUCTION

Leptoquarks (LQ) are exotic particles that have color, electric charge, and lepton number and appear in extended gauge theories and composite models. Current theory suggests that leptoquarks would come in three different generations corresponding to the three quark and lepton generations. Charge 1/3 third generation leptoquarks would decay into either a tau neutrino plus a b quark or, if heavy enough, to a tau lepton plus a t quark.

At the Tevatron, leptoquarks would be produced in pairs through $q\bar{q}$ annihilation or gg fusion, $p+\bar{p} \rightarrow LQ+\overline{LQ}+X$, or singly through the associated lepton production $p+\bar{p} \rightarrow LQ+\bar{l}+X$. The contribution of the second process depends on the LQ-l-q coupling and is smaller. Pair production is independent of this coupling and $q\bar{q}$ annihilation dominates for $M_{LQ} > 100$ GeV. Leptoquarks can be either scalar or vector particles. This analysis sets limits assuming they are scalar for which the cross section is lower and better determined [1]. The current limits on the LQ_3 mass established by the D0 and CDF collaborations based on Fermilab Run I data are 94 GeV [2] and 148 GeV [3] for the $b\bar{b}\nu\bar{\nu}$ final state. A CDF search in the $b\bar{b}\tau\bar{\tau}$ channel gave a limit of 99 GeV [4]. This analysis uses Fermilab Run II data, with $p\bar{p}$ collisions at $\sqrt{s} = 1.96$ TeV, to set new limits for the production of charge 1/3 scalar leptoquark pairs decaying to the $b\bar{b}\nu\bar{\nu}$ final state. The presence of neutrinos are inferred from significant transverse missing energy detected in the event, while the b jets are identified using either the impact parameter of tracks or an associated muon.

II. DATA SAMPLES

Data was collected by the D0 detector [5] using two different jet plus missing energy triggers during different time periods. The first required at least three calorimeter trigger towers with $E_T > 5$ GeV at Level 1 and the vector sum of the jets' transverse energy, defined as $\not{H}_T \equiv |\sum_{jets} \vec{p_t}|$, was required to be > 20 GeV at Level 2 and > 30 GeV at Level 3. A total of 261 pb^{-1} was collected with this trigger. An additional 49 pb^{-1} was collected by also requiring that the acoplanarity, defined as the azimuthal angle between the two leading jets, be $< 169°$ and the scalar sum of jet p_T, H_T, be > 50 GeV. The total sample corresponds to an effective integrated luminosity of 310 pb^{-1}.

III. DEFINITION OF OBJECTS

Electromagnetic (EM) objects are identified using the pattern of energy deposited in the calorimeter while muons are required to have hits in both the muon wire chambers and scintillation counters. The missing transverse energy, $\not{E}_T$, is determined by the vector sum of the transverse components of the energy deposited in the calorimeter and the p_T of detected muons. Jets are reconstructed by a cone algorithm with radius $\Delta R = \sqrt{(\Delta\eta)^2 + (\Delta\phi)^2} = 0.5$ in pseudorapidity (η) and azimuthal angle (ϕ) space about the jet's axis. "Good" jets correspond to the criteria: (a) $0.05 <$ EM fraction < 0.95; (b) the coarse hadronic fraction < 0.4; (c) confirmed by the L1 trigger; and (d) there are no reconstructed EM objects with p_T over 5 GeV in $\Delta R_{EM-jet} < 0.4$.

IV. SIGNAL AND BACKGROUND GENERATION

The signal samples for leptoquark masses 150 - 220 GeV were generated with PYTHIA 6.202 [6]. Instrumental background to our signal comes mostly from QCD multijet processes with $\not{E}_T$ arising from mismeasurement. This background dominates the low $\not{E}_T$ region. Physical backgrounds include processes with real $\not{E}_T$. We define these as SM processes and background from them was estimated using MC events. The most important of them are leptonic decays of W/Z bosons + jets when a lepton remains unreconstructed or is misidentified as a hadron, and processes with a t quark. For all samples the next-to-leading order cross sections were obtained from Ref. [7]. At the parton level the single top MC was generated with COMPHEP 4.4 [8] and ALPGEN [9] was used for all other samples. These events were then processed with PYTHIA, which performed showering and hadronization. An average of 0.8 minimum bias events were superimposed on each MC event. The resulting samples were processed using a full GEANT [10] simulation of the D0 detector. CTEQ5L [11] was used as a parton density function in all cases.

V. b-JET IDENTIFICATION

We used jets which contained tracks with a significant impact paramater, defined by the jet lifetime probability (JLIP) algorithm, or muons to select b-jet candidates and we require two b-tags in each event.

The JLIP b-tagging algorithm uses the fact that tracks originating from secondary vertices have larger impact parameters than tracks from the primary vertex. The algorithm requires at least two tracks in a jet each with a hit in the silicon tracker. The probability of a jet to be of light flavor was calculated and we required this to be $< 2\%$. This gave a b-tag efficiency of about 45%. This value was chosen to maximize the expected mass limits after all other cuts were applied.

A muon tagged a jet if it was within a cone in (η, ϕ) space of $\Delta R_{\mu-jet} < 0.5$ about the jet's axis. Muons originating from K/π decays in general have a softer p_T spectrum than muons from heavy quark decays and we required $p_T^{\mu} > 6$ GeV to suppress their contribution. Backgrounds from W events are due to the isolated muon from the direct decay of a W overlapping with a jet. To suppress such events calorimeter and track isolation cuts were applied. We required $F_{\mu} > 0.7$, with F_{μ} defined as the fraction of calorimeter energy around the muon direction in a 0.4 cone divided by that in a 0.6 cone. We also required that Σp_T^{track}, the sum of track p_T in a cone of 0.5 around the muon, be > 10 GeV, and that the approximate p_T of the muon relative to the jet's axis, $\Delta R_{\mu-jet} \times p_T^{\mu}$, be < 3.5 GeV, as muons originating from jets are closer to the jet axis for higher values of p_T [12]. These cuts are not independent but being combined reduce the W background by 95% while keeping 75% of signal. Muon tagging gave a b-tag efficiency of about 11% with $< 0.5\%$ of light flavored jets passing the tag criteria.

VI. EVENT SELECTION

A. Before b-tagging

A "pretag" sample was selected with the following requirements (Table I). Cuts similar to the trigger conditions, $\not\!\!H_T > 40$ GeV, acoplanarity $< 165°$, and the leading jet having $E_T > 40$ GeV with another jet having $E_T > 20$ GeV, were imposed and both trigger samples were analyzed together. The leading jet was required to have $|\eta| < 1.5$.

We reduced the number of events with mismeasured $\not\!\!E_T$ by requiring the primary vertex be within ± 60 cm in the beam direction from the center of the detector, and by eliminating those events where the $\not\!\!E_T$ vector overlapped a jet in ϕ. This was done by requiring that the $\Delta\phi$ between the direction of $\not\!\!E_T$ and the nearest jet with $E_T > 15$ GeV be > 0.7 and the $\Delta\phi$ between the direction of $\not\!\!E_T$ and the first leading jet is < 3.0. We also rejected events which contained any jet that failed the good jet criteria and had $E_T > 15$ GeV and required track confirmation of all good jets with $E_T > 15$ GeV and $|\eta| < 1.5$. A jet is considered confirmed if the scalar sum of the p_T of tracks associated with it exceeds 5% of the jet E_T. The efficiency of these two jet-related cuts was determined using $W \rightarrow \mu\nu + jets$ events and measured to be 0.95 ± 0.01.

To help reduce the contribution from $W \rightarrow l\nu$ decays, we veto on events with isolated EM objects with $p_T > 5$ GeV or isolated muons with $p_T > 5$ GeV ($p_T > 10$ GeV for muons with poorer momentum resolution). The leptons were required to have $\Delta R_{l-jet} > 0.5$ separation from any jet. We also vetoed events which contain a leading isolated track with $\Delta R_{track-jet} \times p_T > 3.5$ GeV. The track should have $p_T > 5$ GeV and is considered isolated if a hollow cone with an inner radius 0.05 and an outer radius 0.2 around it does not contain any tracks with $p_T > 1.5$ GeV. Finally, $\not\!\!E_T > 70$ GeV and scalar $H_T > 110$ GeV were required. Fig. 1 show distributions of $\not\!\!E_T$ and H_T with the LQ and

TABLE I: Number of data events and expected signal events after different cuts.

Cut description	Data	signal(acceptance), M_{LQ}=200 GeV
trigger, $\not\!\!E_T$ >40 GeV, $\Delta\phi(\not\!\!E_T$,jet) >0.5	482635	59.1 (71.1%)
$\not\!\!H_T > 40$ GeV	445280	58.6 (70.5%)
leading jet $E_T > 40$ GeV	419451	58.3 (70.1%)
second jet $E_T > 20$ GeV	167601	51.7 (62.2%)
no bad jets $E_T > 15$ GeV	91568	49.7 (59.8%)
the primary vertex $\lvert z \rvert < 60$ cm	87873	49.1 (59.1%)
leading jet $\lvert\eta\rvert < 1.5$	69892	47.9 (57.6%)
jet track confirmation	49494	45.9 (55.3%)
no isolated EM objects $p_T > 5$ GeV	46569	45.5 (54.8%)
no isolated muons	44198	45.0 (54.2%)
muon $p_T^{max} < 200$ GeV	44153	44.9 (54.1%)
$\Delta\phi(\not\!\!E_T$,jet) > 0.7	25348	41.6 (50.1%)
acoplanarity $< 165°$	24661	40.6 (48.8%)
$\not\!\!E_T$ >70 GeV	2804	36.5 (43.9%)
$\Delta R \times p_T > 3.5$ GeV, $H_T > 110$ GeV		
$\Delta\phi(\not\!\!E_T$,jet) <3.0	1241	29.9 (35.9%)

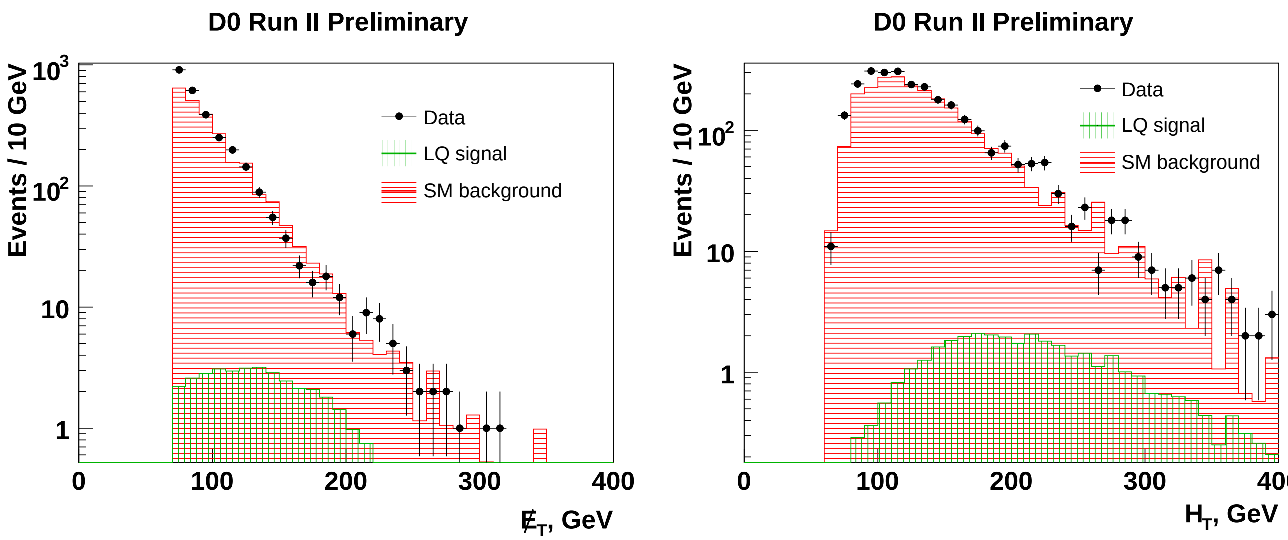

(a) (b)

FIG. 1: (a) The $\not{E}_T$ before b-tagging and (b) the scalar H_T before b-tagging. The points are data, the vertical-hatch are LQ signal events and the horizontal-hatch are SM processes.

SM events normalized to the integrated luminosity. The data sample reproduces the SM expectations which indicates that contributions from other sources, such as QCD multijet processes, are small.

B. b-tagging

Two of the jets in the event were required to be b-tagged. The b-jets in the signal should dominate the energy in the event and the quantity $X_{jj} \equiv (E_T^{tag1} + E_T^{tag2})/(\Sigma_{jets} E_T)$ was defined.

Events which had one or more muon-tagged jets were also required to have at least one JLIP tag (which could be the muon-tagged jet). If this condition was not satisfied then two JLIP b-tags and $X_{jj} > 0.8$ were required. The results of the event selection and the predicted number of events from SM processes are listed in Table II.The largest contributions come from $W/Z + b\bar{b}$ production and top quark signal. For LQ masses above 170 GeV, cuts on $\not{E}_T$

TABLE II: Predicted number of events from SM backgrounds after b-tagging (statistical errors only).

Process	Pretag	double JLIP tag ($\not{E}_T > 90$ GeV,$H_T > 150$ GeV)	Muon + Single JLIP tags ($\not{E}_T > 70$ GeV)	Total
$W \to \mu\nu+$ jj	287 ± 9	0.02 ± 0.01	0.15 ± 0.07	0.17 ± 0.07
$W \to e\nu+$ jj	320 ± 18	0.02 ± 0.01	0 ± 0	0.02 ± 0.01
$W \to \tau\nu+$jj	698 ± 44	0.15 ± 0.04	0 ± 0	0.15 ± 0.04
$Z \to \nu\bar{\nu}+$ jj	1062 ± 21	0.38 ± 0.14	0.03 ± 0.03	0.41 ± 0.14
top	60 ± 1	0.71 ± 0.06	0.80 ± 0.09	1.51 ± 0.11
$W/Z + b\bar{b}$	28 ± 1	0.66 ± 0.07	0.53 ± 0.11	1.19 ± 0.13
total SM expected	2456 ± 53	1.95 ± 0.17	1.52 ± 0.16	3.47 ± 0.24
# data events	2804	1	0	1
Signal (acceptance, %)				
$M_{LQ} = 200$ GeV	37 ± 1 (43.9)	5.8 ± 0.2 (6.9)	3.1 ± 0.2 (3.7)	8.8 ± 0.2 (10.6)

and H_T were optimized as a function of M_{LQ} and applied only to the double JLIP tag sample. Table III presents the final results with the $\sigma(p\bar{p} \to \nu\nu b\bar{b}) \times B^2$ limits obtained using the techniques in [13] with B being the branching fraction into the b quark plus neutrino channel. For higher mass points, one event remains in the data compared to an expected 3 events from SM processes. Fig. 2 show distributions of $\not{E}_T$ and H_T after b-tagging.

Fig. 3 show the cross section limits as a function of M_{LQ}. Limits on the LQ_3 mass were obtained by the intersection of the observed 95% cross section limit with the lower bound of theory for which variation of the renormalization

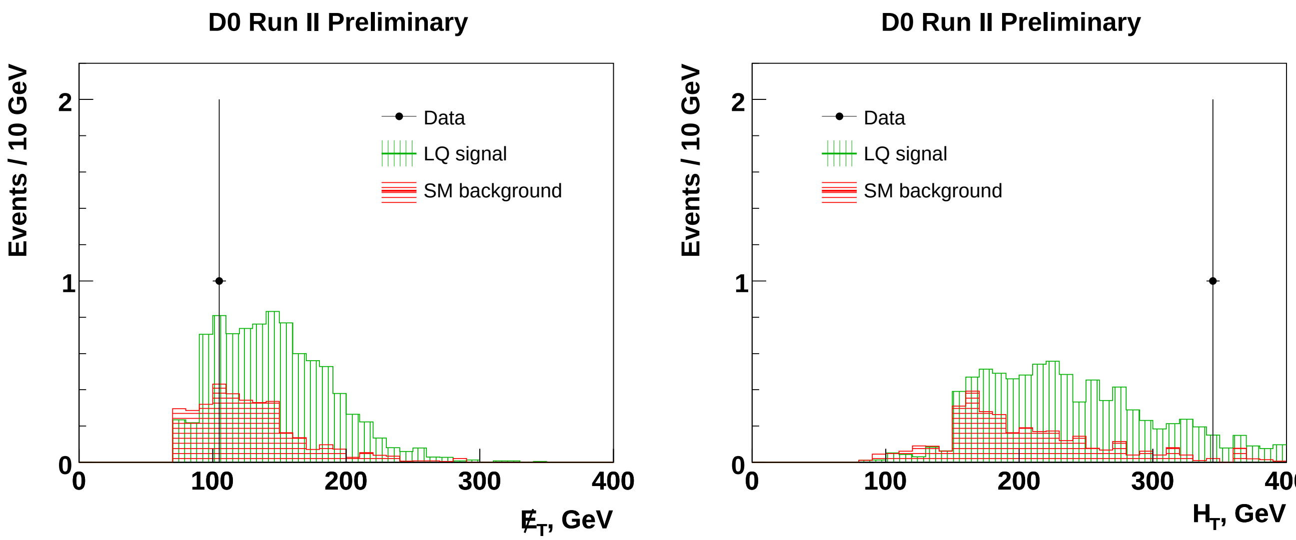

(a) (b)

FIG. 2: (a) The $\not\!\!E_T$ after b-tagging and (b) the scalar H_T after b-tagging. The points are data, the vertical-hatch are LQ signal events and the horizontal-hatch are SM processes.

scale $\mu = \pm 2M_{LQ}$ and the PDF errors were included. If $M(LQ) > M(t) + M(\tau)$ the $LQ \to t\tau$ decay is possible. We assume that the branching fraction for $LQ \to \nu b$ is $1 - 0.5 \times F_{sp}$ where F_{sp} is the phase space suppression factor for the $t\tau$ channel [14]. This is shown on the figure as a displacement from the lower edge of the theory band. The 95% CL cross section limit on leptoquark mass achieved in the analyses is then 213 GeV. If $B(LQ \to \nu b) = 1$ is assumed we obtain a limit of 219 GeV.

TABLE III: Analysis Summary

M_{LQ} GeV	$(\not\!\!E_T,\ H_T)^a$ GeV	Data # events	SM ± stat ± sys # events	Signal ± stat ± sys # events	Accept. %	σ 95% CL limit pb obs/exp
150	(70, 110)	4	5.8 ± 0.3 ± 1.4	39.5±1.1±6.4	8.0±1.2	0.26 / 0.33
160	(70, 110)	4	5.8 ± 0.3 ± 1.4	30.1±0.7±4.8	9.0±1.3	0.23 / 0.29
170	(70, 110)	4	5.8 ± 0.3 ± 1.4	23.3±0.5±3.8	10.0±1.5	0.20 / 0.26
200	(90, 150)	1	3.5 ± 0.2 ± 0.8	8.7±0.2±1.4	10.5±1.6	0.12 / 0.18
220	(90, 190)	1	2.6 ± 0.2 ± 0.6	4.7±0.1±0.8	10.8±1.6	0.12 / 0.15

[a]applied to non-muon subsample only

VII. SYSTEMATIC ERRORS

Sources of systematic uncertainties included errors on the determination of the integrated luminosity and SM cross sections. Trigger and jet selection efficiencies were measured with data and their contribution to the systematic errors was small. The energy of jets (and $\not\!\!E_T$) were varied within the energy scale correction errors and the impact on the signal acceptance and background rates were determined with MC. Errors on the efficiency to tag jets came from two sources. Jets required at least two charged particles in the silicon tracker for the JLIP algorithm. This depended on the jet's location and energy and gave an uncertainty of 3%. Uncertainties in the b-tagging itself gave errors of about 12% for signal and 11% for background which include a 1.5% error due to the $b \to \mu$ branching fraction. Systematic errors are summarized in Table IV.

TABLE IV: Systematic Error Summary; values given in percents.

	Jet energy scale	b-tagging efficiency	Integrated luminosity	SM cross section	Trigger efficiency	Jet selection
Signal[a]	+2.4,-3.2	+13.5,-11.4	6.5		5.0	1.0
SM background	+11.8,7.9	+12.0,-10.7	6.5	15.0		

[a]for $M_{LQ} = 200$ GeV sample

VIII. SUMMARY

Data collected with missing transverse energy triggers were analyzed using both muon and impact parameter b-tagging. After requirements on $\not\!\!E_T$ and double b-tagging, the number of events which passed our selection cuts agreed with the SM expectations. Assuming a decay into the $\nu\bar{\nu}b\bar{b}$ channel, a mass limit of 213 GeV for charge 1/3 third generation leptoquarks was obtained. This limit assumes that $LQ \rightarrow \tau t$ occurs and is suppressed due to phase space. If $B(LQ \rightarrow \nu b) = 1$, then our mass limit is 219 GeV.

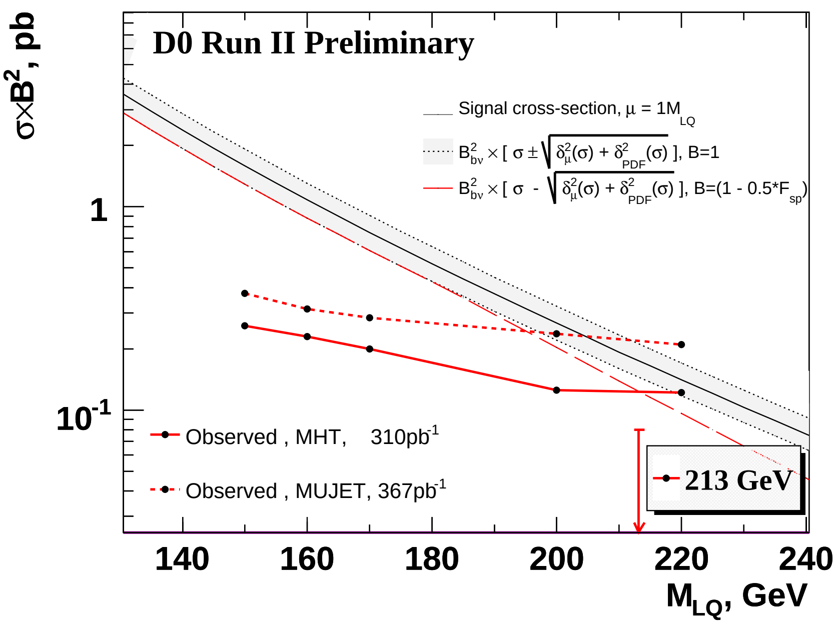

FIG. 3: The 95% CL limit on $\sigma B^2_{b\nu}$ (points plus solid line) as a function of M_{LQ} for the pair production of third generation leptoquarks. The theory band is shown in grey with an error range as discussed in the text. The long-dashed line below the theory band indicates the threshold effect for the τt channel. Also shown are the 95% CL limits obtained using a muon plus jet trigger (points plus short-dashed line) as discussed in the appendix.

Appendix A. Muon plus jet trigger data

A similar analysis was performed using data collected with muon plus jet triggers. The main trigger requirements were the presence of a muon candidate with hits in muon scintillators and wire chambers and a jet with $E_T > 20$ GeV. An integrated luminosity of 367 pb^{-1} was collected with this trigger.

"Preselection" cuts required a muon with $p_T > 4$ GeV and two jets with $E_T > 40$ GeV for the first and $E_T > 20$ GeV for the second. In addition, cuts on $\not\!\!H_T > 50$ GeV, $\not\!\!E_T > 75$ GeV, and $\Delta\phi(\not\!\!E_T, jet) > 0.7$ were applied. Events with isolated EM objects or muons were rejected. One jet was required to have $|\eta| < 1.5$ and the highest E_T non-tagged jet (the "recoil" jet) was required to have $E_T > 50$ GeV. The X_{jj} parameter, which includes the muon p_T, was required to be > 0.8. We then required that there is one muon-tagged jet and at least one JLIP b-tag. No events remained after these cuts. The cut flow is shown in Table V.

TABLE V: Expected number of events for the muon plus jet trigger sample (M_{LQ3} = 150 GeV).

Cut	Data	SM ± stat	Signal (acceptance)	W($\mu\nu$)jj	W/Z($l\nu$)jj	W/Z($l\nu$)$b\bar{b}$	Top^a
Preselection	191	178 ± 9	36.2 (6.2%)	101	37.0	7.45	32.8
e/μ iso. veto	146	143 ± 9	35.7 (6.1%)	86.6	32.9	5.45	17.7
$\|\eta\| < 1.5$	111	110 ± 7	31.8 (5.5%)	65.9	23.8	4.43	16.0
$X_{jj} > 0.8$	76	70 ± 6	26.9 (4.6%)	44.5	18.9	3.33	3.63
$E_T^{rjet} > 50.$	45	41 ± 4	21.3 (3.7%)	28.7	7.01	2.15	3.08
			Muon + Single JLIP b-tag				
	0	2.4 ± 0.3	13.4 (2.3%)	0.2	0.0	1.1	1.1

[a]The SM MC samples are arranged in groups: W($\mu\nu$)jj contains only W($\mu\nu$)jj; W/Z($l\nu$)jj includes all W($e\nu,\tau\nu$)+jj and Z($\nu\nu$)+jj; samplesW/Z($l\nu$)$b\bar{b}$ includes all W($\mu\nu, e\nu, \tau\nu$)+$b\bar{b}$ and Z($\nu\nu$)+$b\bar{b}$; Top contains $t\bar{t}$ and single top samples

The 95% CL limits for the LQ cross section for M_{LQ3} of 150, 160, 180, and 200 GeV are shown in Table VI. The systematic errors on trigger efficiency, jet energy scale corrections, SM cross sections, integrated luminosity and a 6% error due to the $b \rightarrow \mu$ branching fraction are taken into account in the limit determination. A limit on M_{LQ3} of 195 GeV assuming decay into both the νb and τt channels and a limit of 197 GeV assuming $B(LQ \rightarrow \nu b) = 1$ were obtained.

About 70% of signal events which passed the muon plus jet trigger and analysis would also pass the missing energy trigger and analysis described earlier.

TABLE VI: Analysis summary for muon plus jet trigger sample.

M_{LQ3} GeV	Data # events	SM ± stat ± sys # events	Signal ± stat ± sys # events	Accept. %	σ 95% CL limit pb obs(exp)
150	0	2.4±0.3±0.5	13.4±0.9±1.4	2.3±0.3	0.38(0.59)
160	0	2.4±0.3±0.5	10.9±0.5±1.1	2.8±0.2	0.31(0.49)
170	0	2.4±0.3±0.5	8.4 ±0.4±0.9	3.1±0.3	0.29(0.45)
200	0	2.4±0.3±0.5	3.5 ±0.2±0.4	3.6±0.3	0.24(0.37)
220	0	2.4±0.3±0.5	2.1 ±0.1±0.2	4.1±0.3	0.21(0.34)

Acknowledgments

We thank the staffs at Fermilab and collaborating institutions, and acknowledge support from the DOE and NSF (USA); CEA and CNRS/IN2P3 (France); FASI, Rosatom and RFBR (Russia); CAPES, CNPq, FAPERJ, FAPESP and FUNDUNESP (Brazil); DAE and DST (India); Colciencias (Colombia); CONACyT (Mexico); KRF and KOSEF (Korea); CONICET and UBACyT (Argentina); FOM (The Netherlands); PPARC (United Kingdom); MSMT (Czech Republic); CRC Program, CFI, NSERC and WestGrid Project (Canada); BMBF and DFG (Germany); SFI (Ireland); The Swedish Research Council (Sweden); Research Corporation; Alexander von Humboldt Foundation; and the Marie Curie Program.

[1] M. Kramer, T. Plehn, M. Spira and P. M. Zerwas, Phys. Rev. Lett. **79**, 341 (1997).
[2] D0 Collaboration, B. Abbott *et al.*, Phys. Rev. Lett. **81**, 38 (1998).
[3] CDF Collaboration, F. Abe *et al.*, Phys. Rev. Lett. **85**, 20562061 (2000).
[4] CDF Collaboration, F. Abe *et al.*, Phys. Rev. Lett. **78**, 2906 (1997).
[5] D0 Collaboration, V. Abazov *et al.*, "The Upgraded D0 Detector", accepted by NIM.
[6] T. Sjostrand *et al.*, Computer Phys. Commun. 135 (2001) 238.
[7] J.M Campbell and R.K. Ellis , Phys.Rev. D **60**, 113006 (1999);
J.M Campbell and R.K. Ellis , Phys.Rev. D **62**, 114012 (2000).
[8] E. Boos *et al.* [CompHEP Collaboration], Nucl. Instrum. Meth. A **534**, 250 (2004).
[9] M.L Mangano et al., "ALPGEN, generator for hard multiparton processes in hadronic collisions", JHEP 0307 (2003).
[10] A. Agostinelli *et al.*, NIM A 506 (2003), 250-303.

[11] H.L. Lai et al., Eur. Phys. J C12, 375 (2000).
[12] V. Barger and R. Phillips "Collider physics"
Redwood City, Calif. : Addison-Wesley Pub. Co., Advanced Book Program, 1987.
[13] T. Junk, Nucl. Instrum. Meth. A **434**, 435 (1999).
[14] We used $B(LQ \to \nu b) = 1 - 0.5 \times F_{sp}$, where $F_{sp} = \sqrt{(1+d_1-d_2)^2 - 4d_1}[1-(d_1+d_2)/2-(d_1-d_2)^2/2]$, with $d_1 = (m_t/M_{LQ})^2$ and $d_2 = (m_\tau/M_{LQ})^2$. T. Rizzo (private communication).

Extra Figures

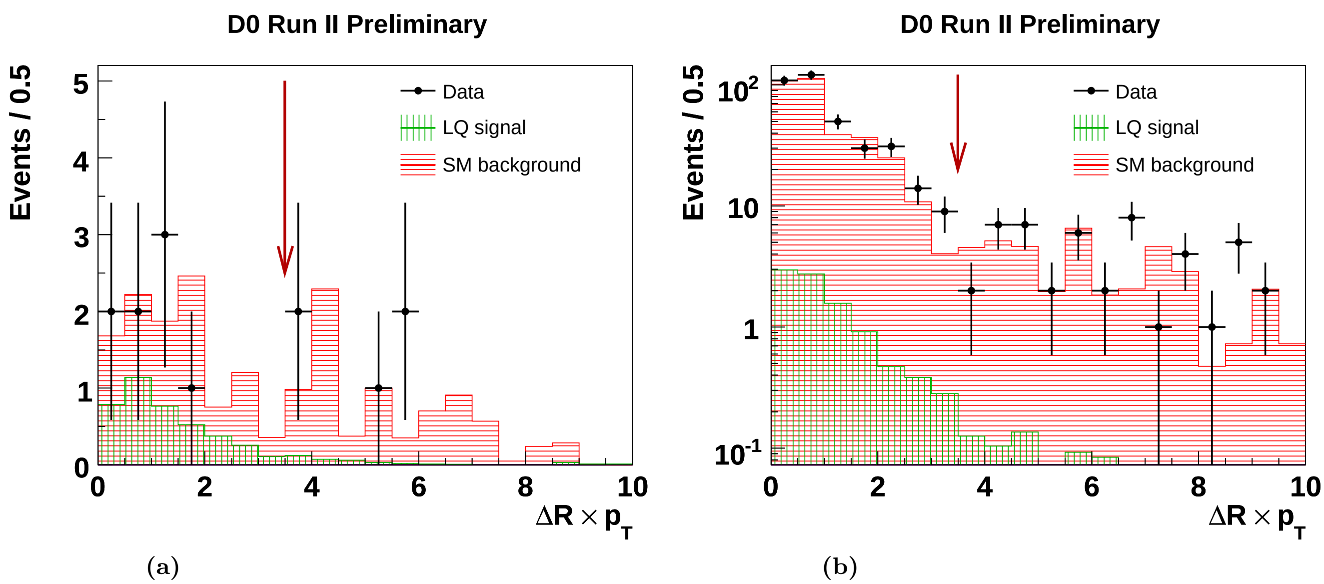

FIG. 4: (a) the approximate p_T of the muon relative to the jet's axis $\Delta R_{\mu-jet} \times p_T^\mu$, (b) $\Delta R_{track-jet} \times p_T$ of the leading isolated track. The points are data, the vertical-hatch are LQ signal events and the horizontal-hatch are SM processes. Arrows corresspond to the applied cuts.

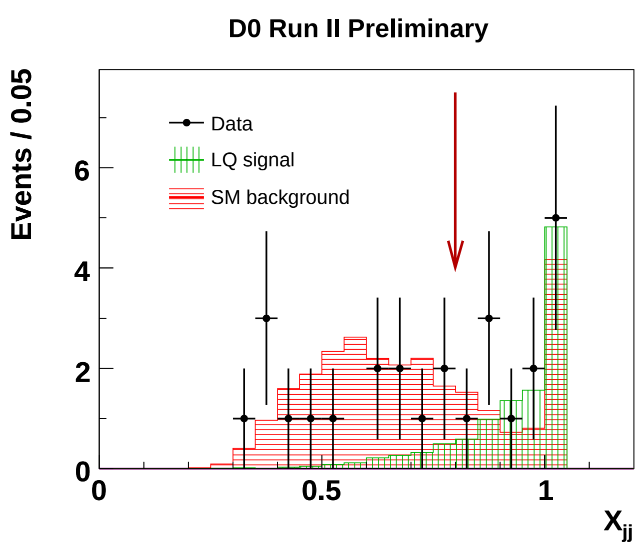

FIG. 5: The distribution of the X_{jj} quantity. The points are data, the vertical-hatch are LQ signal events and the horizontal-hatch are SM processes. An arrow corressponds to the applied cut.